The Journal of Immunology

Proinflammatory Cytokines Disrupt Epithelial Barrier Function by Apoptosis-Independent Mechanisms

Matthias Bruewer, Andreas Luegering, Torsten Kucharzik, Charles A. Parkos, James L. Madara, Ann M. Hopkins and Asma Nusrat

References   This article **cites 69 articles**, 25 of which you can access for free at:
http://www.jimmunol.org/content/171/11/6164.full#ref-list-1

Why *The JI*? Submit online.

- **Rapid Reviews! 30 days*** from submission to initial decision

- **No Triage!** Every submission reviewed by practicing scientists

- **Fast Publication!** 4 weeks from acceptance to publication

*average

Subscription   Information about subscribing to *The Journal of Immunology* is online at:
http://jimmunol.org/subscription

Permissions   Submit copyright permission requests at:
http://www.aai.org/About/Publications/JI/copyright.html

Email Alerts   Receive free email-alerts when new articles cite this article. Sign up at:
http://jimmunol.org/alerts

Proinflammatory Cytokines Disrupt Epithelial Barrier Function by Apoptosis-Independent Mechanisms[1]

Matthias Bruewer,*† Andreas Luegering,*‡ Torsten Kucharzik,*‡ Charles A. Parkos,* James L. Madara,*§ Ann M. Hopkins,* and Asma Nusrat[2]*

It is well known that inflammatory conditions of the intestinal mucosa result in compromised barrier function. Inflammation is characterized by an influx into the mucosa of immune cells that influence epithelial function by releasing proinflammatory cytokines such as IFN-γ and TNF-α. Mucosal barrier function is regulated by the epithelial apical junctional complex (AJC) consisting of the tight junction and the adherens junction. Since the AJC regulates barrier function, we analyzed the influence of IFN-γ and TNF-α on its structure/function and determined the contribution of apoptosis to this process using a model intestinal epithelial cell line, T84, and IFN-γ and TNF-α. AJC structure/function was analyzed by confocal microscopy, biochemical analysis, and physiologic measurement of epithelial gate/fence function. Apoptosis was monitored by determining cytokeratin 18 cleavage and caspase-3 activation. IFN-γ induced time-dependent disruptions in epithelial gate function that were potentiated by coincubation with TNF-α. Tight junction fence function was somewhat disrupted. Cytokine treatment was associated with internalization of AJC transmembrane proteins, junction adhesion molecule 1, occludin, and claudin-1/4 with minimal effects on the cytoplasmic plaque protein zonula occludens 1. Detergent solubility profiles of junction adhesion molecule 1 and E-cadherin and their affiliation with "raft-like" membrane microdomains were modified by these cytokines. Inhibition of cytokine-induced apoptosis did not block induced permeability defects; further emphasizing their primary influence on the epithelial AJC structure and barrier function. Our findings for the first time clearly separate the proapoptotic effects of IFN-γ and TNF-α from their abilities to disrupt barrier function. *The Journal of Immunology,* 2003, 171: 6164–6172.

Abnormal mucosal permeability has been observed in patients with inflammatory bowel disease (IBD),[3] where patients present with relapsing diarrhea attributed to inflammation and altered epithelial paracellular permeability (1–5). Increased paracellular permeability in turn enhances antigenic exposure to underlying immune cells, further compromising barrier function.

Epithelial paracellular permeability is regulated by the apical-most intercellular junctional complex referred to as the apical junctional complex (AJC). The major constituents of the AJC are the tight junction (TJ) and the subjacent adherens junction (AJ). The TJ acts as a gate regulating solute flux and a fence preventing lateral diffusion of proteins and lipids between the outer leaflet of the apical and basolateral plasma membrane domains (6, 7). Proteins constituting the TJ complex include the transmembrane proteins occludin, claudin (CLD) family members and junctional adhesion molecule (JAM), and linker proteins such as zonula occludens 1 (ZO-1) that affiliate with the underlying actin cytoskeleton (8–11). The AJ is immediately subjacent to the TJ and is essential for cell-cell recognition and cell sorting (12). The AJ composition is similar to TJs since it consists of a transmembrane protein (E-cadherin) and cytoplasmic linker proteins (catenin α, β, γ) that affiliate with the underlying actin cytoskeleton (13, 14). Since the TJ and AJ are intimately linked, they are referred to as the AJC.

IFN-γ and TNF-α are both elevated in the mucosa of IBD patients and contribute to the proinflammatory cascade, which includes barrier disruption. Numerous studies have examined IFN-γ- and TNF-α-induced changes in epithelial paracellular permeability. Variable effects of these cytokines on the TJ cytoplasmic plaque protein ZO-1 and TJ structure have been reported (15–22). Given these diverse reports and to understand the mechanisms by which proinflammatory cytokines such as IFN-γ and TNF-α enhance paracellular permeability, we analyzed in detail the influence of these cytokines on the AJC.

Cytokine-induced apoptosis has also been implicated in contributing to compromised mucosal barrier function. Increased apoptosis of colonic crypt cells has been reported in ulcerative colitis and is associated with Fas ligand-expressing lamina propria lymphocytes (23). Moreover, cross-linking of Fas induces apoptosis in diverse cell types including intestinal epithelial cells (24–26). It is still unclear whether this increase in apoptosis compromises barrier function in vivo. Epithelial cell apoptosis and extrusion without loss of barrier function represents a normal physiologic event in the gastrointestinal tract (27). However, exposure of colonic

*Department of Pathology and Laboratory Medicine, Epithelial Pathobiology Research Unit, Emory University, Atlanta, GA, 30322; Departments of †General Surgery and ‡Medicine B, University of Muenster, Muenster, Germany; and §Pritzker School of Medicine, University of Chicago, Chicago, IL

[2] Address correspondence and reprint requests to Dr. Asma Nusrat, Department of Pathology and Laboratory Medicine, Emory University, Whitehead Research Building, Room 105E, 615 Michael Street, Atlanta, GA 30322. E-mail address: anusrat@emory.edu

[3] Abbreviations used in this paper: IBD, inflammatory bowel disease; AJ, adherens junction; AJC, apical junctional complex; CLD, claudin; CTL, control, DIG, detergent-insoluble glycolipid raft; FD-3, fluorescein dextran 3000 Da; JAM-1, junction adhesion molecule 1; TER, transepithelial electrical resistance; TJ, tight junction; ZO-1, zonula occludens 1; ZVAD-fmk, Z-Val-Ala-Asp-fluoromethylketone; TX-100, Triton X-100.

organ cultures to IFN-γ or TNF-α causes a marked increase in Fas sensitivity, indicating that the proinflammatory cytokine microenvironment present in IBD might sensitize the colonic epithelial cells to increased apoptosis (28, 29).

The present study addresses not only the effects of these proinflammatory cytokines on the AJC, but also examines the contribution of cytokine-induced apoptosis to increased paracellular permeability. We present a number of novel aspects in our study including data on time-dependent IFN-γ-induced disruption of epithelial gate and fence function with minimal compromise of epithelial polarity. We observed a differential internalization of TJ transmembrane proteins with minimal effects on the cytoplasmic plaque protein ZO-1. Changes in epithelial permeability were associated with redistribution of JAM-1 from membrane raft-containing fractions. Redistribution of the AJ protein E-cadherin accompanied a change in its biophysical detergent-solubility properties that may be critical for potentiation of IFN-γ-induced permeability changes by TNF-α. Finally, inhibition of apoptosis did not alter the IFN-γ/TNF-α-mediated increase in permeability. These findings provide important clues regarding mechanisms by which proinflammatory, proapoptotic cytokines such as IFN-γ/ TNF-α compromise epithelial barrier function in disease states such as IBD.

Materials and Methods

Cell culture, IFN-γ and TNF-α incubation

T84 epithelial cells (American Type Culture Collection, Manassas, VA) were grown in 1/1 DMEM and Ham's F-12 medium supplemented with 15 mM HEPES (pH 7.5), 14 mM NaHCO$_3$, antibiotics, and 6% NCS (30). T84 cells were seeded on collagen-coated, permeable polycarbonate filters (5-μm pore size) with surface areas of 0.33, 5, or 45 cm^2 (Costar, Cambridge, MA) as described previously (31). TNF-α (10 ng/ml; Genzyme, Cambridge, MA) and IFN-γ (100 U/ml; kind gift from Genentech, San Francisco, CA) were added basolaterally to monolayers for varying periods of time ranging from 5 to 72 h. Alternatively, monolayers were coincubated with TNF-α (10 ng/ml) for the final 5-h incubation with IFN-γ at 24-, 48-, or 72-h time points. Control (CTL) monolayers were incubated with cell culture medium only.

Electrophysiology and permeability assays

All monolayers were checked for high transepithelial electrical resistance (TER) before each experiment using an epithelial voltohmmeter (EVOM/ EndOhm; World Precision Instruments, Sarasota, FL). Paracellular permeability to fluoresceinated dextran 3000 Da (FD-3) was assessed as previously described (32). Briefly, monolayers were washed in HBSS/10 mM HEPES (HBSS$^+$) and equilibrated at 37^{0}C/10 min on an orbital shaker. Monolayers were loaded apically with 1 mg/ml FD-3 (Molecular Probes, Eugene, OR). Basolateral samples were taken at $t = 0$ and 120 min, and fluorescence intensity was analyzed on a fluorescent plate reader (Fluostar; BMG Labtechnologies, Durham, NC). FD-3 concentrations transported into the basolateral compartment were extrapolated from a standard curve and expressed as μM · cm^{-2}·h^{-1} FD-3 transported. Monolayers permeabilized with Triton X-100 (TX-100; 1%) for 10 min were used as positive CTLs.

Apoptosis assays

For detection of apoptotic T84 cells in situ, monolayers were stained with FITC-conjugated M30 Cytodeath Ab (Roche Molecular Biochemicals, Mannheim, Germany), which recognizes cleaved cytokeratin 18. Monolayers washed twice with cold PBS were fixed in methanol for 30 min at −20°C, incubated with an anti-cytokeratin 18 Ab (1/500 dilution) in PBS containing 1%BSA/0.1%Tween 20 (2 h/20°C), and mounted in antiquench medium (Molecular Probes). Apoptosis was quantified by counting the number of M30-positive cells per high-power field. An average of four fields in six samples per condition were counted. For caspase-3 activation, confluent T84 monolayers on 5-cm^2 permeable supports were harvested in lysis buffer and centrifuged at 15,000 $\times$ g for 20 min at 4°C. After equalizing supernatant protein concentrations, caspase-3 activation was measured using the CaspACE Assay System (Promega, Madison, WI) according to the manufacturer's instructions. Wells containing no cell extract served as background CTLs. In some monolayers, the caspase inhibitor

Z-Val-Ala-Asp-fluoromethylketone (ZVAD-fmk, 50 μM; Promega) was added basolaterally with cytokines.

Immunofluorescence labeling

T84 monolayers exposed to medium only, IFN-γ, and/or TNF-α for the indicated periods were washed and fixed/permeabilized in either ethanol at −20°C for 20 min or with 3.7% paraformaldehyde (10 min at room temperature) and 0.5% TX-100. Nonspecific background was blocked with 5% normal goat serum (1 h at room temperature). Monolayers were incubated with primary Abs to occludin (1/400), ZO-1 (1/400), claudin-1 (1/100), claudin-4 (1/100; Zymed Laboratories, San Francisco, CA), JAM-1 (J10.4, 5 μg/ml) (11), E-cadherin (1/100), or β-catenin (1/200; Transduction Laboratories, Lexington, KY) for 1 h. Monolayers were washed and probed with Alexa-Fluor-488 (1/1000; Molecular Probes) or FITC-conjugated (1/ 400; Jackson ImmunoResearch Laboratories, West Grove, PA) secondary Abs. Nuclei were counterstained with TO-PRO-3-iodide (Molecular Probes) and mounted as described above. To visualize ICAM-1 (RR 6.5, 10 μg/ml) (33), carcinoembryonic Ag (1/16000; DAKO, Glostrup, Denmark) and β_1-integrin (10 μg/ml, MAb13, gift from Dr. K. Yamada, National Institutes of Health, Bethesda, MD), double immunolabeling was performed. All monolayers were visualized on an LSM510 confocal microscope (Carl Zeiss Microimaging, Thornwood, NY).

Immunoblotting for AJC proteins in T84 epithelial cells

Confluent T84 monolayers on 5-cm^2 permeable supports were washed in HBSS$^+$ and scraped into extraction buffer (100 mM KCl, 3 mM NaCl, 3.5 mM MgCl$_2$, and 10 mM HEPES, pH 7.4) containing 1% TX-100 with protease inhibitors PMSF (250 μM), leupeptin (5 μg/ml), chymostatin (10 μg/ml), and pepstatin (0.25 μg/ml), aprotinin (2 μg/ml) and phosphatase inhibitors (sodium fluoride, 25 mM; sodium orthovanadate, 10 mM). Cell lysates were centrifuged (1500 $\times$ g for 5 min at 4°C) and equivalent protein concentrations in the postnuclear lysate (10 μg/lane) from CTL and treated monolayers were subjected to SDS-PAGE and Western blot analysis for AJC proteins (37).

Differential detergent extraction of AJC proteins

Confluent monolayers (5 cm^2) of T84 cells were washed and incubated for 30 min at 4°C with 1% TX-100 extraction buffer as above. The TX-100-soluble fraction was subjected to low-speed centrifugation to remove cell debris and added to an equal amount of 2$\times$ sample buffer (3% SDS, 0.75 M Tris (pH 8.8), 20% glycerol, 20 mM DTT). The TX-100-insoluble fraction was scraped into an equal amount of SDS sample buffer. Equal volumes of each fraction were analyzed by SDS-PAGE and immunoblotting for AJC proteins as previously described (34). Densitometry was performed using the UN-SCAN-IT automated digitizing system (Silk Scientific, Orem, UT).

Isolation of detergent-insoluble glycolipid rafts (DIGs)

T84 cells grown on 45-cm^2 permeable supports were harvested into HBSS$^+$ containing 1% TX-100 and protease inhibitors (as above). The sucrose concentration of the cell lysate was adjusted to 40% and placed at the bottom of an ultracentrifuge tube, overlain with a 5–30% (w/w) linear sucrose gradient as previously described (11). Gradients were ultracentrifuged (19 h/39,000 rpm/4°C), fractionated, and analyzed for sucrose concentration, light scattering at 600 nm, protein concentration, and alkaline phosphatase activity as previously described (35, 36). TJ/AJ protein profiles in raft fractions were determined by SDS-PAGE and Western blotting.

Statistics

Results are expressed as mean $\pm$ SEM. Student t test or Welch test was used to compare results, with statistical significance assumed at $p < 0.05$. Individual experiments were performed in triplicate or greater, and each experiment was performed independently three or more times.

Results

Cytokine effects on paracellular permeability

Since the proinflammatory cytokines IFN-γ and TNF-α have been reported to influence epithelial barrier function (18–20, 22), we analyzed their effects on our T84 epithelial monolayers. Confluent T84 monolayers grown on permeable supports were incubated with IFN-γ, TNF-α, or both (combined cytokine treatment) and paracellular permeability was determined by measurement of TER and flux of a paracellular solute, 3-kDa FD-3. In CTL samples or

those incubated with TNF-α alone, TER was maintained at a high value of ~2000 $\Omega \cdot cm^2$. Basolateral incubation with IFN-γ induced a time-dependent fall in TER with a maximum effect at 72 h (Fig. 1A). The TER in these monolayers was reduced from 2074 $\pm$ 52 $\Omega \cdot cm^2$ to 229 $\pm$ 18 $\Omega \cdot cm^2$ after 72-h IFN-γ or to 176 $\pm$ 10 $\Omega \cdot cm^2$ after 72 h of combined cytokine treatment, respectively. These changes in TER were accompanied by a significant increase in paracellular flux of FD-3 (4.3 $\pm$ 0.5 $\mu M \cdot cm^{-2} \cdot h^{-1}$ to 79 $\pm$ 13.1 $\mu M \cdot cm^{-2} \cdot h^{-1}$ after 72-h IFN-γ treatment) (Fig. 1B). The combined cytokine treatment potentiated the effect of IFN-γ on paracellular permeability as noted by the significant increase in FD-3 flux at all time points relative to IFN-γ-treated monolayers. The relative difference in TER drop vs increase in FD-3 flux is consistent with previous reports that have shown exponential increases in flux at TER values <300 $\Omega \cdot cm^2$ (32). Thus, at these TER values, measurement of flux reveals greater sensitivity as a parameter of paracellular transport.

The cytokine treatment protocol used in our studies did not induce irreversible cell necrosis, since cytokine washout was associated with complete TER recovery (data not shown). However, monolayers incubated with a combination of TNF-α and IFN-γ for 72 h did not recover TER (data not shown). Therefore, in all subsequent experiments (unless otherwise stated), TNF-α was added to IFN-γ-treated monolayers for the final 5 h of the IFN-γ incubation period, which was sufficient to increase paracellular permeability relative to IFN-γ-treated monolayers without inducing loss of monolayer integrity. The latter condition is referred to as "combined cytokine" treatment.
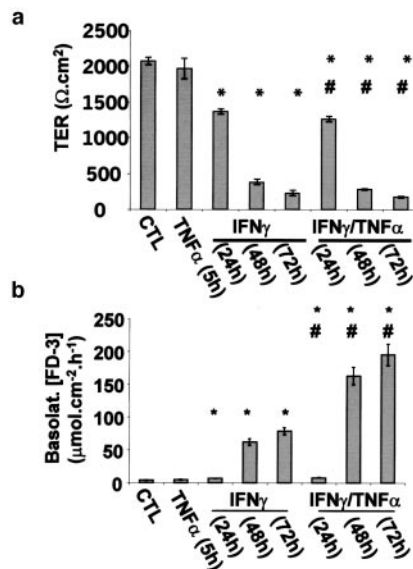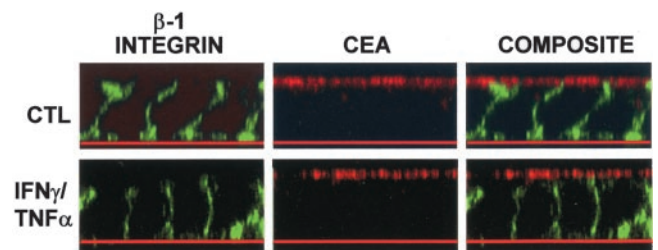

FIGURE 1. Time course of cytokine effects on epithelial barrier function. Barrier function was monitored by measurement of TER and paracellular flux of FD-3. *A,* TER was measured after basolateral incubation of polarized epithelial monolayers with IFN-γ (100 U/ml; up to 72 h), TNF-α (10 ng/ml; 5 h), or both. The graph is an average of six experiments performed in quadruplicate; error bars indicate SEM. Where indicated, TER was significantly less than for CTL (*, $p < 0.0001$) or IFN-γ-treated (#, $p < 0.01$; ##, $p < 0.001$; ###, $p < 0.02$) monolayers at the same time point. *B,* Paracellular flux of FD-3 in confluent T84 monolayers after basolateral exposure to IFN-γ (100 U/ml; up to 72 h), TNF-α (10 ng/ml; 5 h), or both. FD-3 flux is expressed in $\mu mol \cdot cm^{-2} \cdot h^{-1}$ and the graph represents an average of three experiments in quadruplicate with error bars representing SEM. Where indicated, FD-3 flux was significantly higher than for CTL (*, $p < 0.0001$) or IFN-γ-treated (#, $p = 0.02$; ##, $p < 0.0001$) monolayers at the same time point.

Cytokine effects on epithelial polarity

In addition to regulating paracellular ions and solute flux, the TJ also forms a fence preventing lateral diffusion of proteins and lipids (6). We considered whether polarized distribution of membrane proteins in apical/basolateral membranes was disrupted after prolonged cytokine treatment. We examined membrane localization of known epithelial apical markers such as carcinoembryonic Ag and ICAM-1 in parallel with a basolaterally distributed protein, β_1-integrin. Although no apical expression of ICAM-1 was detected in unstimulated T84 cells, cytokine treatment induced ICAM-1 up-regulation that was polarized to the apical membrane. Carcinoembryonic Ag was identified in the apical membranes of both CTL and cytokine-exposed monolayers. β_1-integrin localized exclusively to the lateral membrane of CTL cells with minimal redistribution from the lateral membrane following incubation with IFN-γ with or without TNF-α for 72 h (Fig. 2). These findings suggest minimal repolarization of apical and basolateral plasma membrane proteins of epithelial cells exposed to our proinflammatory cytokines.

Enhanced paracellular permeability after cytokine treatment is not secondary to apoptosis

Since IFN-γ and TNF-α compromise epithelial barrier function and these cytokines reportedly induce apoptosis, (28, 29, 38), we evaluated the contribution of apoptosis to barrier disruption. Two parameters were used to measure cytokine-induced apoptosis. The first involved colorimetric measurement of caspase-3 activity (39–41). Exposure of monolayers to TNF-α for 5 h did not induce increased caspase-3 activity relative to CTL monolayers (Fig. 3A). In contrast, 72-h treatment with IFN-γ and combined cytokine treatment significantly increased caspase-3 activity. Interestingly, coincubation of IFN-γ and TNF-α for 72 h did not further increase caspase-3 activity relative to combined cytokine treatment. Since caspase-3 activation in epithelial cells is associated with cytokeratin 18 cleavage, (42), we immunostained cytokine-incubated monolayers with an Ab (M30) that recognizes the cytokeratin 18 cleavage product. Fig. 3B shows en face confocal images of M30 staining in epithelial cells. Only a few cells in CTL and TNF-α-treated monolayers were positive for M30. Incubation with IFN-γ for 72 h with or without TNF-α for 5 or 72 h increased the number of M30-positive cells. Quantitation revealed significantly more M30-positive cells in IFN-γ-incubated monolayers relative to CTLs or TNF-α-exposed monolayers. However, additive effects on M30 staining were observed by combined cytokine treatment for 72 h (Fig. 3C). In addition to the above measures of apoptosis, we quantitated the number of cell nuclei per high-power field ($\times 40$; Fig. 3D). Incubation of T84 monolayers with IFN-γ or combined cytokine treatment induced partial flattening of epithelial

FIGURE 2. Time course of cytokine effects on epithelial polarity. The distribution of β_1-integrin and carcinoembryonic Ag (CEA) were examined by confocal microscopy in epithelial cells incubated basolaterally with medium or with combined cytokine treatment. Shown here are representative *xz* projections ($\times 100$; scale bar, 10 μm), with filters pseudocolored red.
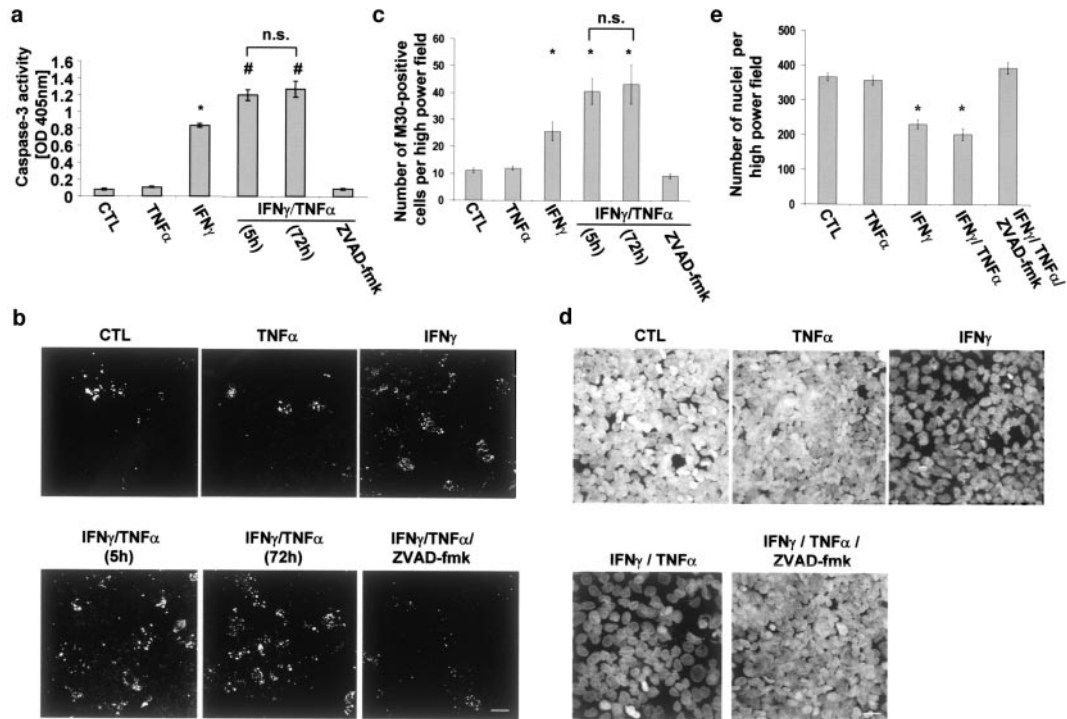
FIGURE 3. Apoptosis is induced by basolateral cytokine incubation. Epithelial apoptosis was monitored by measurement of caspase-3 activity, M30 staining, and morphologic observation of nuclei. Representative results are an average of three experiments in duplicate. Addition of the irreversible general caspase inhibitor ZVAD-fmk (50 μM for 72 h) to IFN-γ- and TNF-α-treated monolayers inhibited the proapoptotic effects of these cytokines (*A–E*). *A,* Caspase-3 activity, as measured using a colorimetric assay, increased after IFN-γ (100 U/ml; 72 h) and combined cytokine treatment. Where indicated, caspase-3 activity was significantly higher in IFN-γ (∗, $p < 0.001$) or IFN-γ plus TNF-α-treated monolayers (5 and 72 h; #, $p < 0.0001$) relative to CTLs. *B,* Basolateral exposure to IFN-γ (100 U/ml; 72 h) with or without TNF-α (10 ng/ml; 5 or 72 h) was associated with increased cytokeratin 18 cleavage, highlighted by cytoplasmic staining for the apoptotic marker M30 in these representative en face confocal micrographs (×40; scale bar, 10 μm). *C,* Quantification of M30-positive cells. As illustrated in the confocal images, T84 cell apoptosis due to caspase cleavage of cytokeratin 18 was increased after IFN-γ (100 U/ml; 72 h) with or without TNF-α (10 ng/ml; 5 or 72 h) treatment. Where indicated, the number of M30-positive cells was significantly higher than CTL (∗, $p < 0.01$). *D,* Epithelial nuclei were highlighted by TO-PRO-3-iodide and visualized by confocal microscopy. IFN-γ with or without TNF-α incubation was associated with apoptosis and extrusion of apoptotic cells. Thus, remaining viable epithelial cells partially spread out, visualized as increased spacing of nuclei between individual cells (×40; scale bar, 10 μm). *E,* Quantification of nuclei remaining after IFN-γ (100 U/ml; 72 h) and combined cytokine treatment. Where indicated, numbers of nuclei were significantly less compared with CTL (∗, $p < 0.0001$).

cells from their normal tall columnar phenotype. This change was accompanied by extrusion of apoptotic cells. Thus, the number of nuclei per field was significantly reduced in monolayers exposed to IFN-γ or combined cytokine treatment (Fig. 3*E*) relative to CTL monolayers or monolayers incubated with TNF-α alone for 5 h. Significantly greater reductions were observed with IFN-γ plus TNF-α treatment for 72 h, with the formation of large spaces between nuclei (data not shown). Since these changes were not associated with increased apoptosis relative to IFN-γ (72 h)/TNF-α (5 h) treatment, but induced irreversible cell damage as determined by a failure to recover TER, it may be that the observed effects were associated with necrotic rather than apoptotic cell damage.

We next examined the influence of an irreversible caspase inhibitor, ZVAD-fmk, on T84 monolayers following combined cytokine treatment. Addition of 50 μM ZVAD-fmk effectively inhibited apoptosis induced by combined cytokine treatment, as examined by caspase-3 activation, cleavage of cytokeratin 18, and nuclear morphology (Fig. 3).

To determine whether cytokine-induced changes in barrier function were related to apoptosis and epithelial cell extrusion, we analyzed the contribution of apoptosis to increased permeability induced by these cytokines. Thus, monolayers were incubated with ZVAD-fmk for 72 h, and the effect of this compound on IFN-γ with or without TNF-α-induced reductions in TER and increase in paracellular flux was determined. As shown in Fig. 4, ZVAD-fmk

by itself did not affect either TER or FD-3 flux and could not reverse effects of combined cytokine treatment on TER and FD-3 flux (Fig. 4). Similarly, ZVAD-fmk blocked apoptosis following coincubation with IFN-γ for 72 h and TNF-α for 72 h, but did not prevent cytokine-induced reductions in barrier function (data not shown). Moreover, double-labeling/confocal microscopy for M30-positive cells and TJ proteins showed that disruption of the latter after cytokine treatment could not be inhibited by ZVAD-fmk (data not shown).

We observed caspase-3 activation at earlier time points of cytokine exposure. However, given the lack of permeability changes at these time points and the inability of ZVAD-fmk to inhibit a cytokine-induced increase in paracellular permeability, we conclude that the permeability effects of our cytokine occur independently of its proapoptotic effects. These findings are consistent with previous reports showing rapid and efficient extrusion of apoptotic epithelial cells without compromise of epithelial barrier function (43).

Cytokines induce redistribution of the AJC

Since epithelial TJs regulate paracellular permeability, we examined the effect of cytokines on organization of candidate TJ proteins by immunofluorescence/confocal microscopy. Epithelial monolayers incubated with IFN-γ for varying time periods up to 72 h with or without TNF-α for the final 5 h were analyzed and
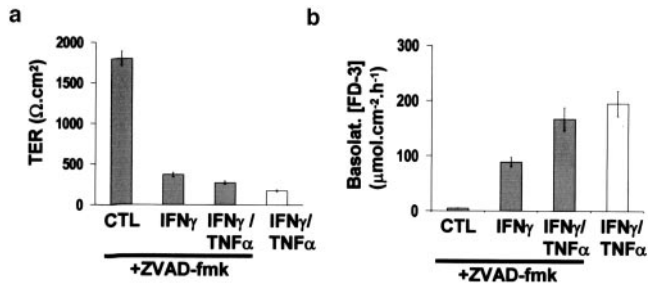
FIGURE 4. Inhibition of apoptosis by the caspase inhibitor ZVAD-fmk does not prevent cytokine-induced barrier disruption. TER (*A*) and paracellular flux (*B*) of FITC-dextran in T84 monolayers exposed basolaterally to medium only (CTL), IFN-γ (100 U/ml; 72 h) alone, or IFN-γ plus TNF-α (10 ng/ml; 5 h) in the presence of ZVAD-fmk. Graph represents three experiments performed in triplicate.

compared with CTL monolayers. In CTLs, the TJ proteins occludin, ZO-1, CLD-1, CLD-4, and JAM-1 were appropriately localized in a chicken wire pattern consistent with their distribution in TJs (Fig. 5, *a–e*). Additionally, a subpool of CLD-1, CLD-4, and JAM-1 was observed further down the lateral membrane (data not
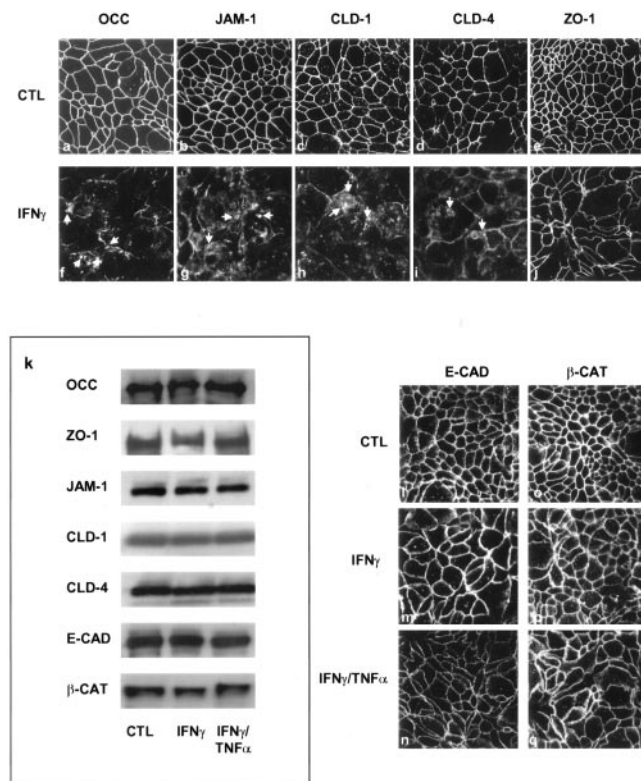
FIGURE 5. Delayed reorganization of AJC proteins following epithelial incubation with cytokines. TJ proteins occludin (OCC), JAM-1, CLD-1, CLD-4, and ZO-1 were localized in CTL monolayers (*a–e*) and in monolayers incubated with IFN-γ for 72 h. IFN-γ exposure (*f–i*) induced dramatic redistribution of occludin, JAM-1, CLD-1, and CLD-4 from the lateral TJ membrane, with internalization (arrows) below the TJ membrane. In contrast to these TJ transmembrane proteins, localization of ZO-1 (*j*) and AJ proteins E-cadherin (E-CAD, *l–n*) and β-catenin (*o–q*) were not significantly changed. Combined cytokine treatment however induced a small decrease in the membrane staining intensity of E-cadherin (*p*) without any major influence on β-catenin localization (*q*). TJ/AJ protein expression as determined by Western blotting was unchanged following cytokine incubation (*k*). Images are representative of four separate experiments (×100; scale bar, 10 μm).

shown). Organization of these proteins in TJs did not change significantly after 24-h cytokine incubation (data not shown).

In contrast to findings at 24 h, incubation of monolayers with IFN-γ alone for 48 h (data not shown) and 72 h induced substantial redistribution of transmembrane proteins occludin, CLD-1, CLD-4, and JAM-1 away from TJs. This change was manifested by discontinuities in membrane staining and submembranous internalization of these proteins (Fig. 5, *f–i*). Despite dramatic redistributions of TJ transmembrane proteins following IFN-γ exposure, the TJ cytoplasmic plaque protein ZO-1 was only minimally affected. In particular, most of the ZO-1 remained at the TJ even after 72 h of IFN-γ incubation (Fig. 5*j*). Combined cytokine treatment did not influence TJ protein organization over observations with IFN-γ alone (data not shown). Cytokine-induced reorganization of TJ proteins was not associated with significant changes in total levels of these proteins as determined by Western blotting, suggesting TJ protein redistribution rather than degradation (Fig. 5*k*). Analysis of subjacent AJ proteins revealed no significant change in E-cadherin and β-catenin distribution following monolayer exposure to IFN-γ (Fig. 5, *l–q*). However, combined cytokine treatment did decrease E-cadherin staining intensity at cell junctions. Analogous to TJ proteins, total cellular levels of AJ proteins were not changed by cytokine exposure (Fig. 5*k*).
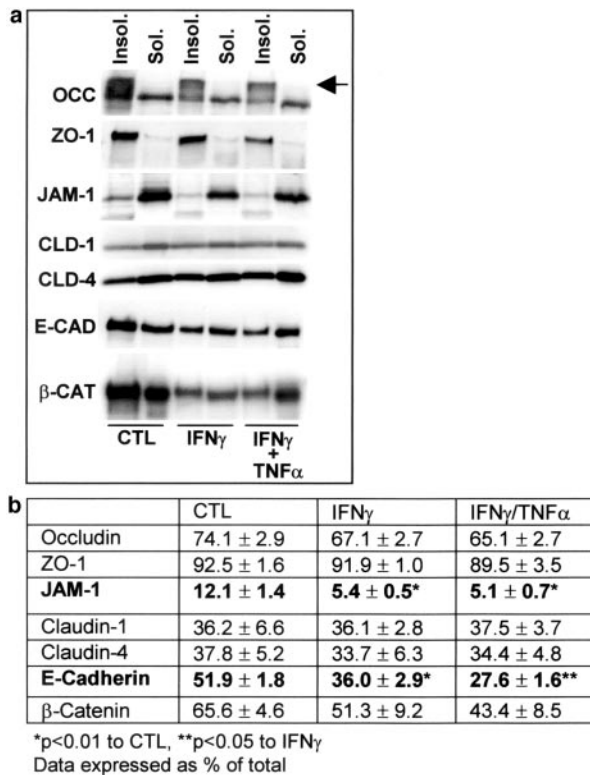
Cytokine influence on detergent solubility of AJC proteins

In epithelial cells with established intercellular junctions, a significant fraction of TJ and AJ proteins partition into a TX-100-insoluble pool that may reflect affiliation with the cytoskeleton or alternatively protein oligomerization (44). Since IFN-γ with or without TNF-α enhanced paracellular permeability and induced TJ/AJ protein redistribution, we analyzed AJC protein TX-100 solubility profiles (Fig. 6*A*). In CTL monolayers, high molecular mass or junction-associated occludin (~80 kDa, arrow) and ZO-1 partitioned predominantly to the TX-100-insoluble pool. IFN-γ exposure for 72 h as well as combined cytokine treatment induced a small decrease in the TX-100-insoluble pool of both occludin and ZO-1. In contrast, CLD-1 and CLD-4 had a significant TX-100-soluble pool. IFN-γ with or without TNF-α treatment had no effect on the TX-100 solubility properties of CLD-1 and CLD-4. Although ~88% of JAM-1 was TX-100 soluble, we observed a reduction in the small TX-100-insoluble pool of JAM-1 after incubation with IFN-γ with or without TNF-α. By immunofluorescence the TX-100-insoluble JAM-1 localized exclusively in TJs and did not extend to the subjacent lateral membrane (data not shown). Densitometry estimating the ratio of the TX-100-insoluble vs soluble pool further emphasized the significant reduction of JAM-1 in the small TX-100-insoluble pool after cytokine treatment, while the ratio for all other TJ proteins was not significantly different (Fig. 6*B*).

The AJ proteins E-cadherin and β-catenin were found in both the TX-100-insoluble and -soluble fractions of CTL and treated monolayers (Fig. 6*A*). We observed a significant shift of E-cadherin toward the TX-100-soluble pool following IFN-γ exposure, potentiated after combined cytokine treatment (Fig. 6*B*). These results suggest that a significant fraction of TX-100-insoluble E-cadherin is affiliated with the actin cytoskeleton and is influenced by cytokine exposure, causing a decrease in cell-cell adhesion.

Cytokines differentially influence affiliation of AJC proteins with membrane rafts

TX-100 insolubility has also been described for proteins partitioning to membrane microdomains or DIGs (35, 45, 46). Since exposure to IFN-γ with or without TNF-α modified the TX-100 solubility profile of TJ proteins and we have previously shown affiliation of TJ proteins with membrane rafts (35), we analyzed

FIGURE 6. Influence of IFN-γ with or without TNF-α on the differential detergent solubility of profiles of AJC proteins. T84 monolayers treated with either IFN-γ (100 U/ml) alone for 72 h or in combination with TNF-α (10 ng/ml; 5 h) were incubated at 4°C with extraction buffer containing 1% TX-100. *A,* The TX-100-soluble (Sol.) and -insoluble (Insol.) fractions were analyzed by SDS-PAGE and immunoblotted for occludin (OCC), ZO-1, CLD-1, CLD-4, JAM-1, E-cadherin (E-CAD), or β-catenin (β-CAT). High molecular mass occludin (arrow) and ZO-1 were predominantly identified in the TX-100-insoluble pools of CTL cells. Similarly, significant pools of the AJ proteins E-cadherin and β-catenin were TX-100 insoluble, whereas CLD-1, CLD-4, and JAM-1 had a significant TX-100-soluble pool. Although incubation with IFN-γ with or without TNF-α did not change the TX-100 solubility profiles of most AJC proteins, we observed a change in the TX-100 insolubility profiles of JAM-1 and E-cadherin. Results of densitometry measurements showing ratios of TX-100-insoluble vs -soluble fractions are shown in *B* as percentage of the TX-100-insoluble pool of the total. A significant change in this ratio was observed for JAM-1 following incubation with IFN-γ with or without TNF-α, emphasizing that the small fraction of JAM-1 in the TX-100-insoluble pool is further diminished by cytokine exposure. Incubation with IFN-γ significantly reduced the TX-100-insoluble pool of E-cadherin and this was further decreased following addition of TNF-α. Results are representative of at least five independent experiments.

the influence of our cytokines on TJ/AJ protein affiliation with membrane rafts. Light scattering at 600 nm, alkaline phosphatase activity, and protein profiles (Fig. 7, *A–C*) were not significantly different in cytokine-treated cells, suggesting that the cytokines did not alter the overall biophysical properties of membrane rafts. The light density DIG fraction (∗) contained only a small proportion of total cellular protein (Fig. 7*C*). However, consistent with our findings in Fig. 7, IFN-γ with or without TNF-α clearly reduced JAM-1 and E-cadherin affiliation with DIGs (Fig. 7*D*). In contrast, associations of other TJ proteins with DIGs were minimally affected.

Discussion

The participation of proinflammatory cytokines in the pathophysiology of IBD is well recognized. Such cytokines have been im-

plicated in epithelial barrier dysfunction (15, 47–49) and in inducing epithelial cell apoptosis (23). Our study was designed to provide a detailed insight into the mechanism(s) by which proinflammatory cytokines IFN-γ and TNF-α compromise epithelial barrier function, and whether or not these are causally linked to apoptosis.

Exposure to IFN-γ evoked time-dependent reductions in epithelial gate function, potentiated by coincubation with TNF-α. It appears that IFN-γ selectively affects paracellular rather than transcellular transport, since it has previously been reported that IFN-γ does not alter transcellular permeability to HRP across epithelial cells (16). Prolonged cytokine treatment also induced subtle deficits in epithelial fence function with minimal effects on polarized distribution of apical vs basal marker proteins. This is in contrast to a study in which mutant Rho GTPases affected both gate and fence function without attendant disruptions in polarity (50).

Since the proinflammatory cytokines used in our study are known to promote apoptosis in different epithelial cell lines (51–54), we addressed the contribution of apoptosis to enhanced paracellular permeability induced by IFN-γ with or without TNF-α. Our results demonstrate that changes in permeability secondary to our cytokine treatments are not directly related to caspase-mediated cell death, since inhibition of apoptosis by ZVAD-fmk did not influence increased paracellular permeability induced by cytokines. Similar results have been described recently in endothelial cells, where ZVAD-fmk inhibited apoptosis but failed to prevent TNF-α-induced increases in permeability (55). In addition, our findings also substantiate observations demonstrating the ability of viable cells to form intercellular junctions and maintain barrier function while apoptotic cells are extruded (43). Despite these findings, it is likely that transient small conductive leaks occur. Others have reported such leaks due to single-cell apoptosis, particularly following incubation with TNF-α (56). Our study shows that inhibition of apoptosis does not block the barrier-disruptive properties of IFN-γ. However, we do not exclude the possibility that permeability defects induced upon prolonged cytokine incubation may be associated with increased cell necrosis. In one study, induction of apoptosis with Fas ligand evoked permeability changes only to small paracellular tracers but not to FD-3 (27). Thus, it could be speculated that permeability deficits induced by IFN-γ are different in nature to those induced by apoptotic stimuli.

A major determinant of TJ function relates to its protein composition in the lateral membrane. We observed dramatic reorganization of TJ proteins in the epithelial lateral membrane, with internalization of transmembrane proteins occludin, CLD-1, CLD-4, and JAM-1 at 48 and 72 h. Redistribution of JAM-1 from intercellular junctions has also been demonstrated in human endothelial cells following treatment with TNF-α and IFN-γ (57). In our study, the cytoplasmic plaque protein ZO-1 maintained its localization at TJs even after 72 h of cytokine treatment. These results conflict somewhat with a previously published report suggesting that IFN-γ-induced permeability changes occur in concert with decreased ZO-1 expression (18). It is intriguing to speculate why ZO-1 localization and expression levels are only slightly affected by our cytokine treatment. ZO-1 is a key TJ cytoplasmic plaque protein that provides a scaffold upon which other proteins can be assembled (58, 59). We hypothesize that ZO-1 maintains its localization to provide this scaffold for efficient reassembly of TJ proteins upon cytokine withdrawal, which would be required for rapid and critical re-establishment of epithelial barrier function. Additionally, a previous report has shown reductions in occludin gene expression induced by TNF-α and IFN-γ in the human intestinal cell line HT-29/B6, suggesting that barrier function could also be affected at gene level (60, 61).

FIGURE 7. Influence of IFN-γ with or without TNF-α on AJC protein association with "raft-like" membrane microdomains. Detergent-insoluble membrane rafts were isolated from T84 cells and the profiles of light scattering at 600 nm (*A*), membrane alkaline phosphatase activity (*B*), and protein concentration (*C*) of CTL monolayers and those treated with IFN-γ (100 U/ml; 72 h) or combined cytokine treatment were determined. Light density TX-100-insoluble complexes (∗) at 22–25% sucrose from CTL and IFN-γ with or without TNF-α exhibit peak light scattering at 600 nm (*A*) and have prominent membrane alkaline phosphatase activity (*B*). Significant changes in the protein profile were not observed following incubation with IFN-γ with or without TNF-α (*C*). *D*, Membrane raft-containing fractions from CTL, IFN-γ-, or IFN-γ plus TNF-α-treated monolayers were analyzed by immunoblotting for occludin (OCC), ZO-1, CLD-1, CLD-4, JAM-1, E-cadherin (E-CAD), and β-catenin (β-CAT) after equalizing for total protein concentration in these fractions. Changes in the profiles of JAM-1 and E-cadherin were observed, reflecting redistribution from raft-containing fractions after incubation of epithelial cells using IFN-γ with or without TNF-α. The above results are representative of three individual experiments.
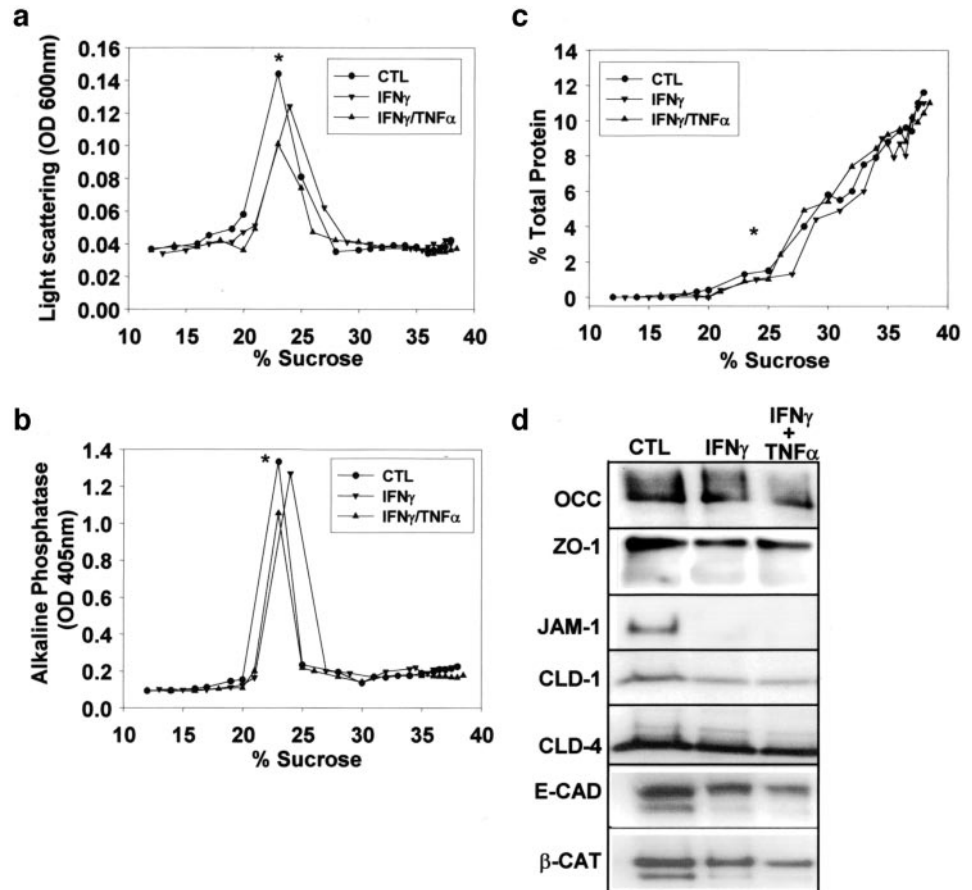
Although by confocal microscopy we too observed dramatic redistribution of TJ transmembrane proteins after IFN-γ with or without TNF-α treatment, we found only modest (if any) biochemical reductions in TX-100-insoluble pools of occludin, ZO-1, CLD-1, and CLD-4. In contrast to the minimal influence of our cytokines on the TX-100-insoluble pools of most TJ proteins, we observed a differential and significant change in JAM-1 partitioning into this small TX-100-insoluble fraction. In the lateral epithelial membrane, JAM-1 is organized not only in TJs but the majority is present in the subjacent lateral membrane of AJ, which is TX-100 soluble. So far, the function of the TX-100-soluble pool of JAM-1 is unknown. Our results suggest that the small TX-100-insoluble TJ-affiliated pool of JAM-1 may be a major target for proinflammatory cytokines.

We have previously shown that TX-100-insoluble TJ proteins are enriched in specific membrane microdomains exhibiting the properties of lipid rafts (35). Moreover, we demonstrated that disassembly of TJs induced by *Clostridium difficile* toxins modified TJ protein association with membrane rafts (36). Considering changes in paracellular permeability and structural reorganization of the AJC, we sought to further explore the effects of IFN-γ with or without TNF-α on AJC protein affiliation with rafts. Despite dramatic increases in paracellular permeability and redistribution of transmembrane TJ proteins after IFN-γ with or without TNF-α treatment, affiliations of most TJ proteins with membrane rafts were not appreciably altered. Interestingly, we observed a decrease in JAM-1 affiliation with TX-100-insoluble membrane rafts. The functional significance of altered JAM-1 expression in membrane rafts may relate to its status as a putative target for pathogens such as reovirus (62). For example, if infectivity of reovirus depends upon the localization of JAM-1 in membrane rafts at the cell sur-

face, then IFN-γ-induced redistribution from membrane rafts may reduce accessibility of such a virus to its target.

Although there were few morphological changes in AJ proteins E-cadherin and β-catenin, biochemically we noted a significant shift of E-cadherin into the TX-100-soluble pool following cytokine exposure. This would support the notion that the lateral membrane pool of E-cadherin involved in mediating cell-cell adhesion is the TX-100-insoluble pool, and cytokine-induced modulation of this pool influences the strength of cell-cell adhesion. This could exacerbate deficiencies in cell-cell adhesion, occurring in concert with alterations in the adjoining TJs. Moreover, the additive effect of TNF-α on paracellular permeability in IFN-γ-incubated monolayers could be partially due to an additional shift of E-cadherin into the TX-100-soluble pool, suggesting that changes in E-cadherin biophysical properties further reduce cell adhesion. Several reports have indicated that IFN-γ can up-regulate expression of TNF-α receptors at both the mRNA and protein level in epithelial and endothelial cells (22, 63–65). Therefore, it is possible that the ability of TNF-α to potentiate the biological effects of IFN-γ maybe secondary to increased signaling from up-regulated TNF-α receptors.

Redistribution of AJC proteins has been observed in tissues from patients with active IBD (66, 67), in which proinflammatory cytokines such as IFN-γ and TNF-α are elevated. The specificity of these mediators for disruption of specific intercellular junctional proteins under inflammatory conditions is indicated by the fact that alterations in all junctional proteins were not observed in noninflamed areas of diseased tissue (66, 67). Despite the fact that apoptosis is increased in IBD (23), our model suggests that permeability defects induced by IFN-γ/TNF-α are separable from their proapoptotic effects.

Although inflamed tissues in vivo secrete a complex milieu of both pro- and anti-inflammatory mediators and cytokines, we speculate that TJ protein redistribution induced by IFN-γ does not reflect a global phenomenon, but rather the effects of a specific cytokine with a key role in the pathology of IBD. Alterations in the distribution of key TJ proteins have been reported in response to hepatocyte growth factor in renal epithelial cells (68) and IL-4/IL-13 in lung epithelial cells, (69); however, we (unpublished results) and others did not observe any alterations in intestinal epithelial cells exposed to the same cytokines (17, 34).

In conclusion, we have analyzed mechanisms by which IFN-γ and TNF-α alter barrier properties of the intestinal epithelium. We report for the first time that increased epithelial paracellular permeability induced by these cytokines is separate from their pro-apoptotic effects and associated with AJC protein restructuring. This scenario is therefore amenable to rapid recovery of epithelial barrier function following reductions of cytokines in the intestinal milieu as inflammation subsides.

Acknowledgments

References

1. Katz, K. D., D. Hollander, C. M. Vadheim, C. McElree, T. Delahunty, V. D. Dadufalza, P. Krugliak, and J. I. Rotter. 1989. Intestinal permeability in patients with Crohn's disease and their healthy relatives. *Gastroenterology* 97:927.
2. Sandle, G. I., N. Higgs, P. Crowe, M. N. Marsh, S. Venkatesan, and T. J. Peters. 1990. Cellular basis for defective electrolyte transport in inflamed human colon. *Gastroenterology* 99:97.
3. Teahon, K., P. Smethurst, A. J. Levi, I. S. Menzies, and I. Bjarnason. 1992. Intestinal permeability in patients with Crohn's disease and their first degree relatives. *Gut* 33:320.
4. May, G. R., L. R. Sutherland, and J. B. Meddings. 1993. Is small intestinal permeability really increased in relatives of patients with Crohn's disease? *Gastroenterology* 104:1627.
5. Irvine, E. J., and J. K. Marshall. 2000. Increased intestinal permeability precedes the onset of Crohn's disease in a subject with familial risk. *Gastroenterology* 119:1740.
6. van Meer, G., and K. Simons. 1986. The function of tight junctions in maintaining differences in lipid composition between the apical and the basolateral cell surface domains of MDCK cells. *EMBO J.* 5:1455.
7. Diamond, J. M. 1977. Twenty-first Bowditch Lecture: the epithelial junction: bridge, gate, and fence. *Physiologist* 20:10.
8. Furuse, M., T. Hirase, M. Itoh, A. Nagafuchi, S. Yonemura, and S. Tsukita. 1993. Occludin: a novel integral membrane protein localizing at tight junctions. *J. Cell Biol.* 123:1777.
9. Furuse, M., M. Itoh, T. Hirase, A. Nagafuchi, S. Yonemura, and S. Tsukita. 1994. Direct association of occludin with ZO-1 and its possible involvement in the localization of occludin at tight junctions. *J. Cell Biol.* 127:1617.
10. Fanning, A. S., B. J. Jameson, L. A. Jesaitis, and J. M. Anderson. 1998. The tight junction protein ZO-1 establishes a link between the transmembrane protein occludin and the actin cytoskeleton. *J. Biol. Chem.* 273:29745.
11. Liu, Y., A. Nusrat, F. J. Schnell, T. A. Reaves, S. Walsh, M. Pochet, and C. A. Parkos. 2000. Human junction adhesion molecule regulates tight junction resealing in epithelia. *J. Cell Sci.* 113:2363.
12. Gumbiner, B. 1990. Generation and maintenance of epithelial cell polarity. *Curr. Opin. Cell Biol.* 2:881.
13. Gumbiner, B. M. 1996. Cell adhesion: the molecular basis of tissue architecture and morphogenesis. *Cell* 84:345.
14. Dejana, E., M. Corada, and M. G. Lampugnani. 1995. Endothelial cell-to-cell junctions. *FASEB J.* 9:910.
15. Schmitz, H., M. Fromm, C. J. Bentzel, P. Scholz, K. Detjen, J. Mankertz, H. Bode, H. J. Epple, E. O. Riecken, and J. D. Schulzke. 1999. Tumor necrosis factor-α (TNFα) regulates the epithelial barrier in the human intestinal cell line HT-29/B6. *J. Cell Sci.* 112:137.
16. Adams, R. B., S. M. Planchon, and J. K. Roche. 1993. IFN-γ modulation of epithelial barrier function: time course, reversibility, and site of cytokine binding. *J. Immunol.* 150:2356.
17. McKay, D. M., and P. K. Singh. 1997. Superantigen activation of immune cells evokes epithelial (T84) transport and barrier abnormalities via IFN-γ and TNFα: inhibition of increased permeability, but not diminished secretory responses by TGF-β2. *J. Immunol.* 159:2382.
18. Youakim, A., and M. Ahdieh. 1999. Interferon-γ decreases barrier function in T84 cells by reducing ZO-1 levels and disrupting apical actin. *Am. J. Physiol.* 276:G1279.
19. Madara, J. L., and J. Stafford. 1989. Interferon-γ directly affects barrier function of cultured intestinal epithelial monolayers. *J. Clin. Invest.* 83:724.
20. Sugi, K., M. W. Musch, M. Field, and E. B. Chang. 2001. Inhibition of Na$^+$,K$^+$-ATPase by interferon γ down-regulates intestinal epithelial transport and barrier function. *Gastroenterology* 120:1393.
21. Taylor, C. T., A. L. Dzus, and S. P. Colgan. 1998. Autocrine regulation of epithelial permeability by hypoxia: role for polarized release of tumor necrosis factor α. *Gastroenterology* 114:657.
22. Fish, S. M., R. Proujansky, and W. W. Reenstra. 1999. Synergistic effects of interferon γ and tumour necrosis factor α on T84 cell function. *Gut* 45:191.
23. Strater, J., I. Wellisch, S. Riedl, H. Walczak, K. Koretz, A. Tandara, P. H. Krammer, and P. Moller. 1997. CD95 (APO-1/Fas)-mediated apoptosis in colon epithelial cells: a possible role in ulcerative colitis. *Gastroenterology* 113:160.
24. Ashkenazi, A., and V. M. Dixit. 1998. Death receptors: signaling and modulation. *Science* 281:1305.
25. Lin, E., J. A. Katz, S. E. Calvano, S. M. Coyle, S. Randhawa, I. Shahin, A. Kumar, and S. F. Lowry. 1998. The influence of human endotoxemia on CD95-induced apoptosis. *Arch. Surg.* 133:1322.
26. Peter, M. E., and P. H. Krammer. 1998. Mechanisms of CD95 (APO-1/Fas)-mediated apoptosis. *Curr. Opin. Immunol.* 10:545.
27. Abreu, M. T., A. A. Palladino, E. T. Arnold, R. S. Kwon, and J. A. McRoberts. 2000. Modulation of barrier function during Fas-mediated apoptosis in human intestinal epithelial cells. *Gastroenterology* 119:1524.
28. O'Connell, J., M. W. Bennett, K. Nally, G. C. O'Sullivan, J. K. Collins, and F. Shanahan. 2000. Interferon-γ sensitizes colonic epithelial cell lines to physiological and therapeutic inducers of colonocyte apoptosis. *J. Cell. Physiol.* 185:331.
29. Ruemmele, F. M., P. Russo, J. Beaulieu, S. Dionne, E. Levy, M. J. Lentze, and E. G. Seidman. 1999. Susceptibility to FAS-induced apoptosis in human nontumoral enterocytes: role of costimulatory factors. *J. Cell. Physiol.* 181:45.
30. Madara, J. L., J. Stafford, K. Dharmsathaphorn, and S. Carlson. 1987. Structural analysis of a human intestinal epithelial cell line. *Gastroenterology* 92:1133.
31. Madara, J. L., C. Parkos, S. Colgan, R. J. MacLeod, S. Nash, J. Matthews, C. Delp, and W. Lencer. 1992. Cl$^-$ secretion in a model intestinal epithelium induced by a neutrophil-derived secretagogue. *J. Clin. Invest.* 89:1938.
32. Sanders, S. E., J. L. Madara, D. K. McGuirk, D. S. Gelman, and S. P. Colgan. 1995. Assessment of inflammatory events in epithelial permeability: a rapid screening method using fluorescein dextrans. *Epithelial Cell Biol.* 4:25.
33. Rothlein, R., M. Czajkowski, M. M. O'Neill, S. D. Marlin, E. Mainolfi, and V. J. Merluzzi. 1988. Induction of intercellular adhesion molecule 1 on primary and continuous cell lines by pro-inflammatory cytokines: regulation by pharmacologic agents and neutralizing antibodies. *J. Immunol.* 141:1665.
34. Nusrat, A., C. A. Parkos, A. E. Bacarra, P. J. Godowski, C. Delp-Archer, E. M. Rosen, and J. L. Madara. 1994. Hepatocyte growth factor/scatter factor effects on epithelia: regulation of intercellular junctions in transformed and nontransformed cell lines, basolateral polarization of c-met receptor in transformed and natural intestinal epithelia, and induction of rapid wound repair in a transformed model epithelium. *J. Clin. Invest.* 93:2056.
35. Nusrat, A., C. A. Parkos, P. Verkade, C. S. Foley, T. W. Liang, W. Innis-Whitehouse, K. K. Eastburn, and J. L. Madara. 2000. Tight junctions are membrane microdomains. *J. Cell Sci.* 113:1771.
36. Nusrat, A., C. von Eichel-Streiber, J. R. Turner, P. Verkade, J. L. Madara, and C. A. Parkos. 2001. *Clostridium difficile* toxins disrupt epithelial barrier function by altering membrane microdomain localization of tight junction proteins. *Infect. Immun.* 69:1329.
37. Parkos, C. A., S. P. Colgan, M. S. Diamond, A. Nusrat, T. W. Liang, T. A. Springer, and J. L. Madara. 1996. Expression and polarization of intercellular adhesion molecule-1 on human intestinal epithelia: consequences for CD11b/CD18-mediated interactions with neutrophils. *Mol. Med.* 2:489.
38. Gitter, A. H., K. Bendfeldt, H. Schmitz, J. D. Schulzke, C. J. Bentzel, and M. Fromm. 2000. Epithelial barrier defects in HT-29/B6 colonic cell monolayers induced by tumor necrosis factor-α. *Ann. NY Acad. Sci.* 915:193.
39. Nicholson, D. W., A. Ali, N. A. Thornberry, J. P. Vaillancourt, C. K. Ding, M. Gallant, Y. Gareau, P. R. Griffin, M. Labelle, Y. A. Lazebnik, et al. 1995. Identification and inhibition of the ICE/CED-3 protease necessary for mammalian apoptosis. *Nature* 376:37.
40. Salvesen, G. S., and V. M. Dixit. 1997. Caspases: intracellular signaling by proteolysis. *Cell* 91:443.
41. Thornberry, N. A., and Y. Lazebnik. 1998. Caspases: enemies within. *Science* 281:1312.
42. Caulin, C., G. S. Salvesen, and R. G. Oshima. 1997. Caspase cleavage of keratin 18 and reorganization of intermediate filaments during epithelial cell apoptosis. *J. Cell Biol.* 138:1379.
43. Madara, J. L. 1990. Maintenance of the macromolecular barrier at cell extrusion sites in intestinal epithelium: physiological rearrangement of tight junctions. *J. Membr. Biol.* 116:177.
44. Wong, V. 1997. Phosphorylation of occludin correlates with occludin localization and function at the tight junction. *Am. J. Physiol.* 273:C1859.
45. Brown, D. A., and J. K. Rose. 1992. Sorting of GPI-anchored proteins to glycolipid-enriched membrane subdomains during transport to the apical cell surface. *Cell* 68:533.
46. Anderson, R. G., and K. Jacobson. 2002. A role for lipid shells in targeting proteins to caveolae, rafts, and other lipid domains. *Science* 296:1821.
47. Coyne, C. B., M. K. Vanhook, T. M. Gambling, J. L. Carson, R. C. Boucher, and L. G. Johnson. 2002. Regulation of airway tight junctions by proinflammatory cytokines. *Mol. Biol. Cell* 13:3218.
48. Greig, E., and G. I. Sandle. 2000. Diarrhea in ulcerative colitis: the role of altered colonic sodium transport. *Ann. NY Acad. Sci.* 915:327.

49. Schmitz, H., C. Barmeyer, A. H. Gitter, F. Wullstein, C. J. Bentzel, M. Fromm, E. O. Riecken, and J. D. Schulzke. 2000. Epithelial barrier and transport function of the colon in ulcerative colitis. *Ann. NY Acad. Sci. 915:312.*

50. Jou, T. S., E. E. Schneeberger, and W. J. Nelson. 1998. Structural and functional regulation of tight junctions by RhoA and Rac1 small GTPases. *J. Cell Biol. 142:101.*

51. Abreu-Martin, M. T., A. Vidrich, D. H. Lynch, and S. R. Targan. 1995. Divergent induction of apoptosis and IL-8 secretion in HT-29 cells in response to TNF-α and ligation of Fas antigen. *J. Immunol. 155:4147.*

52. Mullin, J. M., C. W. Marano, K. V. Laughlin, M. Nuciglio, B. R. Stevenson, and P. Soler. 1997. Different size limitations for increased transepithelial paracellular solute flux across phorbol ester and tumor necrosis factor-treated epithelial cell sheets. *J. Cell Physiol. 171:226.*

53. Soler, A. P., C. W. Marano, M. Bryans, R. D. Miller, L. A. Garulacan, S. K. Mauldin, T. D. Stamato, and J. M. Mullin. 1999. Activation of NF-κB is necessary for the restoration of the barrier function of an epithelium undergoing TNF-α-induced apoptosis. *Eur. J. Cell Biol. 78:56.*

54. Wright, K., G. Kolios, J. Westwick, and S. G. Ward. 1999. Cytokine-induced apoptosis in epithelial HT-29 cells is independent of nitric oxide formation: evidence for an interleukin-13-driven phosphatidylinositol 3-kinase-dependent survival mechanism. *J. Biol. Chem. 274:17193.*

55. Petrache, I., A. D. Verin, M. T. Crow, A. Birukova, F. Liu, and J. G. Garcia. 2001. Differential effect of MLC kinase in TNF-α-induced endothelial cell apoptosis and barrier dysfunction. *Am. J. Physiol. 280:L1168.*

56. Gitter, A. H., K. Bendfeldt, J. D. Schulzke, and M. Fromm. 2000. Leaks in the epithelial barrier caused by spontaneous and TNF-α-induced single-cell apoptosis. *FASEB J. 14:1749.*

57. Ozaki, H., K. Ishii, H. Horiuchi, H. Arai, T. Kawamoto, K. Okawa, A. Iwamatsu, and T. Kita. 1999. Cutting edge: combined treatment of TNF-α and IFN-γ causes redistribution of junctional adhesion molecule in human endothelial cells. *J. Immunol. 163:553.*

58. Wittchen, E. S., J. Haskins, and B. R. Stevenson. 1999. Protein interactions at the tight junction: actin has multiple binding partners, and ZO-1 forms independent complexes with ZO-2 and ZO-3. *J. Biol. Chem. 274:35179.*

59. Itoh, M., M. Furuse, K. Morita, K. Kubota, M. Saitou, and S. Tsukita. 1999. Direct binding of three tight junction-associated MAGUKs, ZO-1, ZO-2, and ZO-3, with the COOH termini of claudins. *J. Cell Biol. 147:1351.*

60. Mankertz, J., J. S. Waller, B. Hillenbrand, S. Tavalali, P. Florian, T. Schoneberg, M. Fromm, and J. D. Schulzke. 2002. Gene expression of the tight junction protein occludin includes differential splicing and alternative promoter usage. *Biochem. Biophys. Res. Commun. 298:657.*

61. Mankertz, J., S. Tavalali, H. Schmitz, A. Mankertz, E. O. Riecken, M. Fromm, and J. D. Schulzke. 2000. Expression from the human occludin promoter is affected by tumor necrosis factor α and interferon γ. *J. Cell Sci. 113:2085.*

62. Barton, E. S., J. C. Forrest, J. L. Connolly, J. D. Chappell, Y. Liu, F. J. Schnell, A. Nusrat, C. A. Parkos, and T. S. Dermody. 2001. Junction adhesion molecule is a receptor for reovirus. *Cell 104:441.*

63. Ruggiero, V., J. Tavernier, W. Fiers, and C. Baglioni. 1986. Induction of the synthesis of tumor necrosis factor receptors by interferon-γ. *J. Immunol. 136:2445.*

64. Bebo, B. F., Jr., and D. S. Linthicum. 1995. Expression of mRNA for 55-kDa and 75-kDa tumor necrosis factor (TNF) receptors in mouse cerebrovascular endothelium: effects of interleukin-1β, interferon-γ and TNF-α on cultured cells. *J. Neuroimmunol. 62:161.*

65. Carrel, S., F. Hartmann, S. Salvi, H. Albrecht, M. Schreyer, and D. Rimoldi. 1995. Expression of type A and B tumor necrosis factor (TNF) receptors on melanoma cells can be regulated by dbc-AMP and IFN γ. *Int. J. Cancer 62:76.*

66. Kucharzik, T., S. V. Walsh, J. Chen, C. A. Parkos, and A. Nusrat. 2001. Neutrophil transmigration in inflammatory bowel disease is associated with differential expression of epithelial intercellular junction proteins. *Am. J. Pathol. 159:2001.*

67. Gassler, N., C. Rohr, A. Schneider, J. Kartenbeck, A. Bach, N. Obermuller, H. F. Otto, and F. Autschbach. 2001. Inflammatory bowel disease is associated with changes of enterocytic junctions. *Am. J. Physiol. 281:G216.*

68. Grisendi, S., M. Arpin, and T. Crepaldi. 1998. Effect of hepatocyte growth factor on assembly of zonula occludens-1 protein at the plasma membrane. *J. Cell Physiol. 176:465.*

69. Ahdieh, M., T. Vandenbos, and A. Youakim. 2001. Lung epithelial barrier function and wound healing are decreased by IL-4 and IL-13 and enhanced by IFN-γ. *Am. J. Physiol. 281:C2029.*